Mycol Progress (2011) 10:323–332
DOI 10.1007/s11557-010-0705-2

ORIGINAL ARTICLE

Ectomycorrhizae associated with *Castanopsis fargesii* (Fagaceae) in a subtropical forest, China

Qin Wang · Cheng Gao · Liang-Dong Guo

Received: 7 July 2010 / Revised: 17 August 2010 / Accepted: 25 August 2010 / Published online: 10 September 2010

Abstract Ectomycorrhizal (ECM) trees were commonly distributed in subtropical forest ecosystems, but we know little of below-ground ECM status. The ECM community composition and anatomical structure of *Castanopsis fargesii* were investigated in a subtropical evergreen broad-leaved forest of southwest China. Twelve root samples of *C. fargesii* were collected from a 2-ha plot and a total of 19 ECM morphotypes were obtained based on morphological characters. Furthermore, a total of 17 ECM fungi were identified from the 19 morphotypes based on the analysis of ITS sequences. Of these fungi, 14 belonged to Basidiomycetes and 3 were Ascomycetes. Taxa in Russulaceae and Thelephoraceae were frequent. *Lactarius* sp., *Russula* sp.1, *Tomentella* sp.2 and *Boletus* sp. were the dominant fungi occurred in more than four samples with importance values of 31.5, 29.4, 23.4 and 22.9%, respectively. The other 13 ECM fungi were rare. Anatomical structures of the 17 ECMs were described. This is the first study to characterize the below-ground ECM communities and anatomical structures in a subtropical evergreen broad-leaved forest.

Keywords Ectomycorrhizal fungi · Diversity · Molecular identification · Castanopsis fargesii

Q. Wang · C. Gao · L.-D. Guo (✉)
Key Laboratory of Systematic Mycology & Lichenology, Institute of Microbiology, Chinese Academy of Sciences, Beijing 100101, People's Republic of China
e-mail: guold@sun.im.ac.cn

Q. Wang · C. Gao
Graduate University of Chinese Academy of Sciences, Beijing 100049, People's Republic of China

Introduction

Ectomycorrhizae (ECM) are symbiotic structures formed between soil fungi and plant roots. The ECM fungi exchange soil-derived nutrients for carbohydrates from the host plants and are beneficial to host species in resistance to abiotic or biotic stresses (Smith and Read 2008). ECM plants are dominant or common species in many natural forests, ECM fungi therefore play important ecological roles in nutrient transportation, inter- or intra-specific interactions, and maintenance of biodiversity in ecosystems (Simard et al. 1997). Understanding the ECM fungal community composition of their hosts is key to understanding the ecology and function of fungus–plant associations in natural ecosystems.

ECM fungal community composition has been widely studied in temperate and boreal forests, and high diversities of ECM fungi were discovered (Gao and Yang 2010; Gebhardt et al. 2007; Smith et al. 2007; Wang and Guo 2010). Recently, there have been some studies of ECM fungal community composition conducted in tropical forests (Haug et al. 2005; Peay et al. 2010; Tedersoo et al. 2007). However, to our knowledge, there has been no study of the below-ground ECM fungal community composition in subtropical evergreen broad-leaved forests, except for the information on community composition based on a fruit-body survey (Liang et al. 2007).

Investigations of ECM fungal communities only based on above-ground fruit bodies cannot provide a complete picture of ECM communities in natural ecosystems (Gardes and Bruns 1996; Grogan et al. 2000). This is because although fruit-bodies are necessarily associated with ectomycorrhizae, a fungus-forming ectomycorrhiza may not always form sporocarps, which are affected by biotic and abiotic factors in natural ecosystems (Horton and Bruns 2001). Advances in molecular techniques have

allowed consistent identification of ECM fungi and have facilitated research in natural ecosystems (Peter et al. 2008). Molecular studies on ECM communities have been widely carried out in temperate and boreal ecosystems (Ishida et al. 2009; Wang and Guo 2010), as well as in tropical regions (Morris et al. 2008; Peay et al. 2010). Although many important ECM trees occur in subtropical forests, we know little of below-ground ECM fungal community composition in these ecosystems.

Subtropical evergreen broad-leaved forests are widespread in south China with high plant diversity and are dominated by ECM trees, suggesting a high richness of these symbioses in the natural ecosystems. Understanding ECM community in abundance, diversity, and anatomical structures is key to understanding the ecology and evolutionary context of fungus–plant associations in natural ecosystems. *Castanopsis fargesii* Franch. (Fagaceae), widely distributed in subtropical regions, is an important ECM tree with significant ecological and economical values in China. However, nothing is known about below-ground ECM community composition and anatomical structures on the roots of *C. fargesii*.

The basic aims of this study were (1) to investigate the below-ground ECM fungal community composition associated with roots of *C. fargesii* based on the analyses of morphology and ITS sequences, and (2) to describe the anatomical structures of ectomycorrhizae of this economically important tree in natural evergreen broad-leaved forest of subtropical region, China.

Materials and methods

Site and sampling procedure

This study was carried out in a 2-ha plot of a natural subtropical evergreen broad-leaved forest in Dujiangyan of Sichuan Province, southwest China (30°44'N, 103°27'E). The site has a mean annual precipitation of 1,244 mm, a mean annual temperature of 15.2°C, and an altitude of 780 m asl. This forest is dominated by evergreen broad-leaved trees, e.g., species of Lauraceae, Fagaceae, and Theaceae. The study was carried out in August 2007. A total of 12 individuals of *C. fargesii* were randomly selected and the distances between individuals were more than 20 m. One root sample was collected from each individual by tracing from trunks of *C. fargesii*. Root samples were taken to laboratory for further analyses.

ECM morphotyping and anatomical structure observation

Root samples were washed free of soil material over a 380-μm sieve in running tap water. Fine roots (<2 mm diam.) of *C. fargesii* were picked manually from each washed sample and were trimmed into ca. 2-cm-long sections. The mycorrhizal system was examined by SMZ-B2 stereomicroscopy (Chongqing Optec Optical Instrument, Chongqing, China). Live ECM root tips were divided into different morphotypes based on general appearance, such as color, luster, size, ramification type and texture, as well as the presence and color of emanating hyphae and rhizomorphs. In each morphotype, no more than three health ECM tips encountered were placed in a 1.5-mL microcentrifuge tube and stored at −20°C for DNA analysis, and the remains were stored in FAA for anatomical observation. Anatomical structures, such as mantle layers, rhizomorphs, cystidia and emanating hyphae, were described according to the keys of Agerer (1986–2006, 2006) and the online key DEEMY (http://www.deemy.de). Plan views were taken at ×20–45 magnification, and mantle structures and cross-section characteristics were recorded at ×1,000 magnification with Nomarski differential interference contrast. More than 20 ECM systems were observed for each morphotype.

DNA extraction, amplification and sequencing

The DNA was extracted according to the protocol of Gardes and Bruns (1993). The ITS (ITS1, 5.8 S, ITS2) regions of rDNA from each ECM morphotype was amplified by PCR using the primer pair ITS1-F/ITS-4B or ITS1-F/ITS-4 (Gardes and Bruns 1993; White et al. 1990) in a PTC 100^{TM} Programable Thermal Controller (MJ Research, USA). The final 50 μL reaction mixture contained 1 μL of template DNA, 1× PCR buffer, 2.0 mM $MgCl_2$, 0.2 mM each dNTP, 15 *p*mol of each primer, and 2.5 U *Taq* polymerase (TransGen Biotech, Beijing, China). The amplification was programmed for a denaturation at 95°C for 5 min, followed by 35 cycles of denaturation for 40 s at 94°C, annealing for 50 s at 50°C, extension for 1 min at 72°C, and a final 10 min extension at 72°C. A negative control using sterile Milli-Q water instead of template DNA was included in the amplification process. Three to five ECM samples of each morphotype were selected for DNA extraction and ITS sequence analysis.

The PCR products were purified using UNIQ-10 PCR production purification kit (Shanghai Sangon Biological Engineering Technology & Services, Shanghai, China) according to manufacturer's instruction. The PCR products were sequenced using ABI Prism 3700 Genetic Analyzer (Applied Biosystems, USA).

Data analysis

A value of 97% ITS region identity was used as a DNA barcoding threshold. This cut-off level is based on error rates generated by PCR, sequencing and inter-specific

variability within ITS regions as employed in other studies using ITS sequences for ECM fungal species identification from roots and soil (Tedersoo et al. 2008). The ITS sequences generated in this study were used as query sequences to search similar sequences in NCBI, EMBL and UNITE databases (Kõljalg et al. 2005) to provide at least tentative identification for the ECM fungi.

Relative frequency is the total number of occurrence of a species divided by the total number of occurrence of all taxa. The relative abundance is the root tip number of a species divided by the total root tip number of all taxa. The relative frequency and relative abundance for each species were then summed for an importance value indicated as a percentage (Horton and Bruns 2001).

Results

ECM fungal community composition

A total of 19 ECM morphotypes were obtained from 2,690 cm of fine roots of *C. fargesii* collected from the 12 samples based on morphological characters. Identical ITS sequences were obtained from the three to five samples of each morphotype. Total 17 ECM fungi were identified from the 19 morphotypes based on the analyses of ITS sequences (Table 1). Of these ECM fungi, 3 were Ascomycetes and 14 belonged to Basidiomycetes. In the Basidiomycetes, 1 was identified at species (*Russula lepida*), 12 at genus level (1 *Boletus* sp., 2 *Clavulina* spp., 1 *Lactarius* sp., 2 *Russula* spp., 2 *Thelephora* spp., and 4 *Tomentella* spp.) and 1 at family (Russulaceae) level. In the Ascomycetes, 2 were identified at ordinal level (Helotiales) and 1 at class level (Sordariomycetes). An average of 2.9 ECM fungi was found per root sample with a range from 1 to 4.

Russulaceae and Thelephoraceae were the most frequent fungi which existed in ten and eight soil samples, respectively. *Lactarius* sp., *Russula* sp. 1, *Tomentella* sp. 2, and *Boletus* sp. were the dominant fungi occurred in more than four samples with important values of 31.5, 29.4, 23.4 and 22.9, respectively. The other 13 ECM fungi were detected less than four soil samples with low importance values (<20%) (Fig. 1).

ECM morphological–anatomical structure

Thelephora sp.1 Morphology: monopodial-pinnate, orange-brown or brown, mantle surface loosely woolly, up to 9.6 mm long, 0.22–0.28 mm diam. Unramified ends bent, tapering to the tip, up to 2.7 mm long, 0.20–0.24 mm diam (Fig. 2a). *Cross-section*: mantle 11–23 μm thick, mantle cells 10–17(20)×2–4 μm, including 4–7 hyphal layers. Hartig's net surrounds half to one and a half rows of cortical cells with a single chain of irregular hyphae, hyphae 2–4 μm diam (Fig. 3a). *Mantle in plane view*: outer layers pseudoparenchymatous, cells polygonal or irregular, 5–

Table 1 Molecular identification of ectomycorrhizal fungi on root tips of *Castanopsis fargesii* based on ITS sequences

ECM fungus	GenBank accession No.	Closest blast match (GenBank accession No.)	Query/reference ITS length (similarity %)
Boletus sp.	GQ900530	*Boletus citrinovirens* (DQ066405)	644/611 (84.0)
Clavulina sp. 1	GQ900529	*Clavulina* sp. (EF417799)	566/574 (90.1)
Clavulina sp. 2	GQ900528	*Clavulina cristata* (EU819415)	577/586 (92.0)
Helotiales sp. 1	GQ900526	Helotiales sp. (AM181410)	477/475 (96.9)
Helotiales sp. 2	GQ900525	Helotiales sp. (FM180478)	474/474 (97.7)
Lactarius sp.	GQ900535	*Lactarius camphorates* (DQ422009)	621/614 (94.4)
Russula lepida	GQ900531	*Russula lepida* (AF418641)	582/577 (98.1)
Russula sp. 1	GQ900534	*Russula amoenipes* (AY061656)	598/602 (91.7)
Russula sp. 2	GQ900532	*Russula amoenipes* (AY061656)	612/602 (92.9)
Russulaceae sp.	GQ900533	*Russula ilicis* (AY061682)	575/559 (84.0)
Sordariomycetes sp.	GQ900524	Sordariales sp. (GQ268554)	488/488 (89.6)
Thelephora sp. 1	GQ900541	*Thelephora terrestris* (EU427330)	576/575 (95.0)
Thelephora sp. 2	GQ900540	*Thelephora* sp.(EF655695)	570/572 (88.2)
Tomentella sp. 1	GQ900539	*Tomentella* sp. (EF619832)	564/564 (95.0)
Tomentella sp. 2	GQ900538	*Tomentella* sp. (EU529972)	578/577 (97.1)
Tomentella sp. 3	GQ900537	*Tomentella* sp. (AM159590)	580/578 (94.3)
Tomentella sp. 4	GQ900536	*Tomentella* sp. (FN185989)	580/577 (88.7)

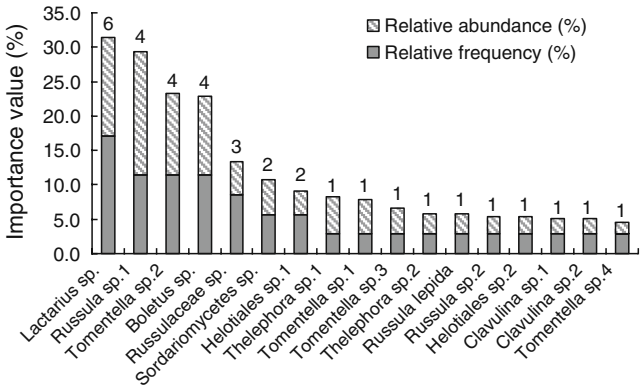

Fig. 1 Ectomycorrhizal fungus community composition in *Castanopsis fargesii*. *Numbers* above the *bars* represent the number of samples in which the fungus was observed

25×5–12 μm (Fig. 4a-1). Inner layers plectenchymatous, hypha cells cylindrical, 2–4 μm diam (Fig. 4a-2).

Thelephora sp.2 Morphology: irregularly monopodial-pinnate, yellow-brown, mantle surface loosely cottony, up to 8.7 mm long, 0.27–0.36 mm diam. Unramified ends bent or sinuous, tapering to the tip, 0.27–1.6×0.18–0.24 mm (Fig. 2b). *Cross-section*: mantle 15–23 μm thick, mantle cells 3–11×2–4 μm, including 6–9 hyphal layers. Hartig's net surrounds one row of cortical cells with a single chain of hyphae, hyphae 2–5 μm diam (Fig. 3b). *Mantle in plane view*: outer layers plectenchymatous, hyphae parallel, 3–4 μm diam (Fig. 4b-1). Middle and inner layers plectenchymatous, hyphae parallel, cylindrical, 3–5 μm diam (Fig. 4b-2, b-3).

Tomentella sp.1 Morphology: monopodial-pinnate (three orders), dark-brown to black, mantle surface loosely cottony, up to 16 mm long, 0.29–0.38 mm diam. Unramified ends straight or bent, tapering to the tip, 0.27–1.8×0.18–0.27 mm (Fig. 2c). *Cross-section*: mantle 13–20 μm thick, mantle cells (2)5–13(18)×2–6 μm, including 3–4 hyphal layers. Hartig's net patchy, nest–like, surrounds one and a half rows of cortical cells with a single chain of hyphae, hyphae 2–5 μm diam (Fig. 3c). *Mantle in plane view*: outer and middle layers pseudoparenchymatous, menbranaceously yellow, cells blunt angular to roundish, 7–22×5–14 μm (Fig. 4c-1, c-2). Inner layers plectenchymatous, menbranaceously yellow to brown, hyphae irregularly arranged, no pattern recognizable, hyphae 3–4(7) μm diam (Fig. 4c-3).

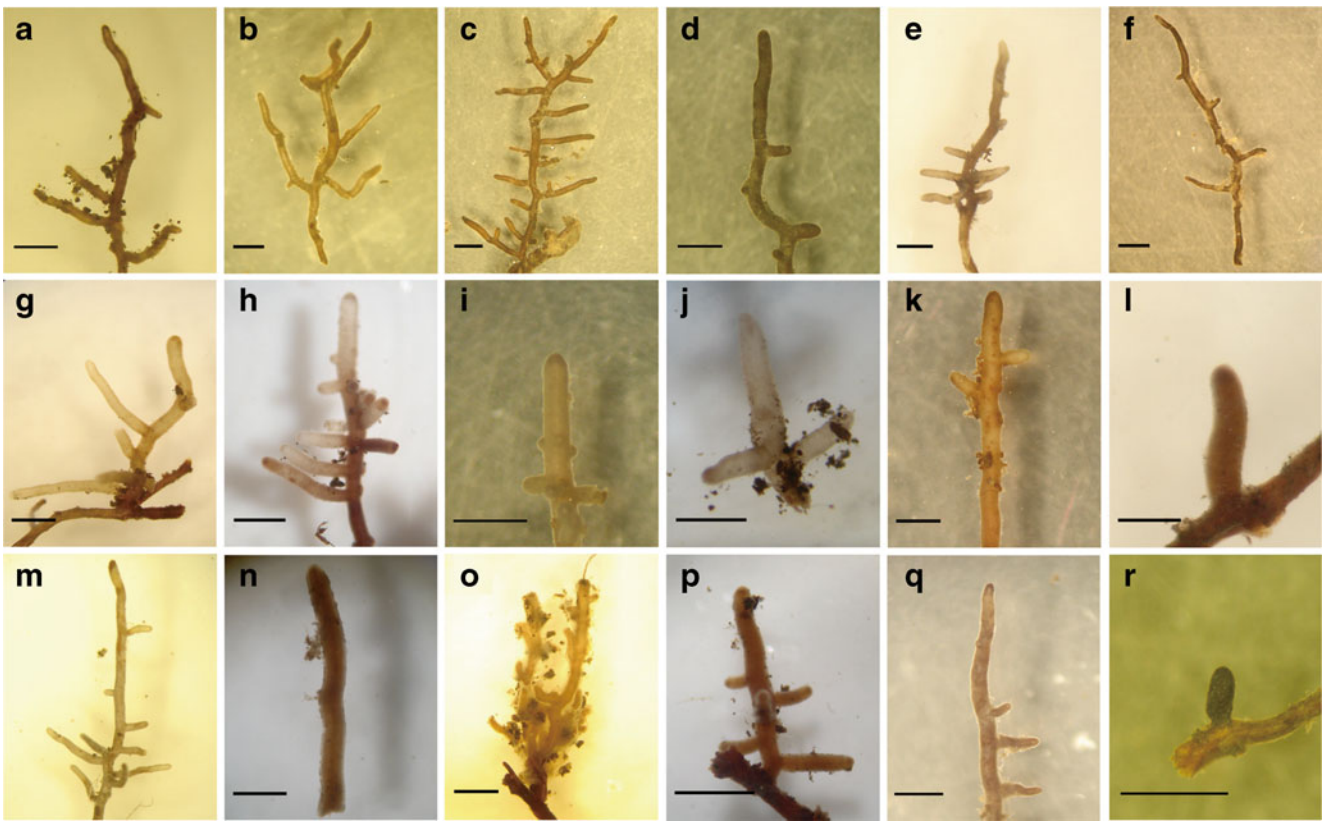

Fig. 2 Plan views of ectomycorrhizas on roots of *Castanopsis fargesii*. **a** *Thelephora* sp.1; **b** *Thelephora* sp.2; **c** *Tomentella* sp.1; **d** *Tomentella* sp.2; **e** *Tomentella* sp.3; **f** *Tomentella* sp.4; **g** *Lactarius* sp.; **h**, **i** *Russula* sp.1; **j** *Russula* sp.2; **k** *Russula lepida*; **l** Russulaceae sp.; **m** *Boletus* sp.; **n** *Clavulina* sp.1; **o** *Clavulina* sp.2; **p** Helotiales sp.1; **q** Helotiales sp.2; **r** Sordariomycetes sp. (*Bar* 1 mm)

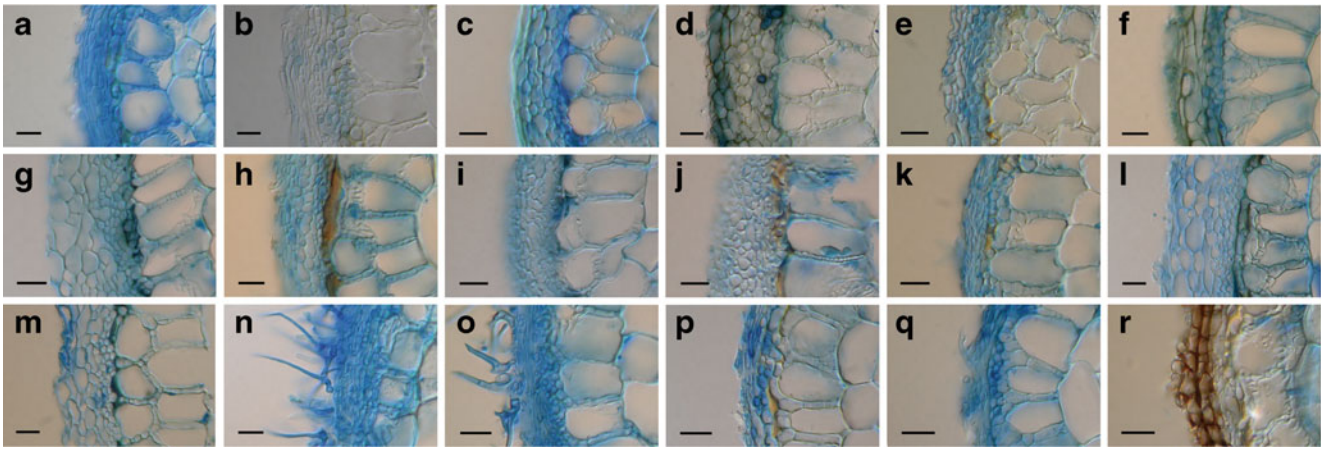

Fig. 3 Anatomical features of ectomycorrhizas in cross-sections. **a** *Thelephora* sp.1; **b** *Thelephora* sp.2; **c** *Tomentella* sp.1; **d** *Tomentella* sp.2; **e** *Tomentella* sp.3; **f** *Tomentella* sp 4; **g** *Lactarius* sp.; **h** *Russula* sp.1; **i** *Russula* sp.2; **j** *Russula lepida*; **k** Russulaceae sp.; **l** *Boletus* sp.; **m** *Clavulina* sp.1; **n**, **o** *Clavulina* sp.2; **p** Helotiales sp.1; **q** Helotiales sp.2; **r** Sordariomycetes sp. (*Bar* 10 μm)

Tomentella sp.2 Morphology: irregularly monopodial, dark-brown to black, mantle surface grainy or warty, up to 7.8 mm long, 0.31–0.38 mm diam. Unramified ends straight or bent, cylindrical, 0.20–1.6×0.20–0.27 mm (Fig. 2d). *Cross-section*: mantle (17)20–32 μm thick, mantle cells 3–20×3–13 μm, including 4–7 hyphal layers. Hartig's net surrounds one and a half rows of cortical cells with a single chain of hyphae, hyphae 2–4 μm diam (Fig. 3d). *Mantle in plane view*: outer layers pseudoparenchymatous, menbranaceously brown, rosette-like, cells polygonal, 5–20×6–11 μm (Fig. 4d-1). Middle layers pseudoparenchymatous, menbranaceously brown, cells blunt polygonal to elongated, 10–23×8–15 μm (Fig. 4d-2). Inner layers plectenchymatous, menbranaceously brown, with sparse, stellately branching hyphae, hyphae 3–6 μm diam (Fig. 4d-3). *Cysitidia*: bottle-shaped, with a strongly inflated bade and a long torn out neck (Fig. 4d-4).

Tomentella sp.3 Morphology: monopodial-pyromidial, yellow to brown, up to 9.1 mm long, 0.20–0.33 mm diam. Unramified ends straight or bent, 0.40–3.3×0.16–0.20 mm (Fig. 2e). *Cross-section*: mantle 15–23 μm thick, mantle cells 3–18×2–5 μm, including 4–6 hyphal layers. Hartig's net surrounds two to three rows of cortical cells with a single chain of hyphae, hyphae 2–4 μm diam (Fig. 3e). *Mantle in plane view*: outer layers plectenchymatous, cells cylindrical to strongly inflated, hyphae 3–8 μm diam (Fig. 4e-1). Middle layers plectenchymatous, cells cylindrical or irregular, 4–8 μm diam (Fig. 4e-2). Inner layers plectenchymatous, cells oblong, rectangular or irregular, 2–5 μm diam (Fig. 4e-3).

Tomentella sp.4 Morphology: monopodial-pinnate, brown, orange-brown to dark brown, up to 20 mm long, 0.22–0.38 mm diam. Unramified ends bent, tapering to the tip, 0.22–2.9×0.16–0.22 mm, mantle surface loosely cottony (Fig. 2f). *Cross-section*: mantle 12–24 μm thick, including 3–4 hyphal layers, mantle cells 2–17(20)×2–8 μm. Hartig's net patchy, nest-like, surrounded one and a half rows of cortical cells with a single chain of hyphae, hyphae 2–5 μm diam (Fig. 3f). *Mantle in plane view*: outer layers pseudoparenchymatous, menbranaceously yellow-brown, cells blunt angular, 8–17×4–12 μm (Fig. 4f-1). Middle layers pseudoparenchymatous, cells menbranaceously yellow-brown, blunt polygonal, 7–20×8–13 μm (Fig. 4f-2). Inner layers plectenchymatous, hyphae parallel, loosely arranged, 2–4 μm diam (Fig. 4f-3). *External hyphae*: with clamps, 2–4 μm diam (Fig. 4f-4).

Lactarius sp. Morphology: monopodial-pinnate or monopodial-pyramidal, yellowish, brown to dark-brown, surface smooth, up to 6.7 mm long, 0.27–0.31 mm diam. Unramified ends straight, up to 2.0 mm long, 0.18–0.24 mm diam (Fig. 2g). *Cross-section*: mantle 30–50 μm thick, cells 2–14(18)×2–8 μm. Hartig's net surrounds one and a half rows of cortical cells with a single chain of elongate hyphae, hyphae 3–5 μm diam (Fig. 3g). *Mantle in plane view*: outer layers pseudoparenchymatous, cells blunt polygonal, roundish, elongated, cells 7–20(28)×6–14 μm (Fig. 4g-1). Middle layers pseudoparenchymatous, cells roundish, elongated, 10–24×7–17 μm (Fig. 4g-2). Inner layers plectenchymatous with irregularly arranged hyphae, hyphae 3–6 μm diam (Fig. 4g-3).

Russula sp.1 Morphology: mostly monopodial-pyramidal, occasionally unbranched, whitish to brown or red-brown, mantle surface smooth, up to 6.2 mm long, 0.27–0.38 mm diam. Unramified ends straight, cylindrical, 0.18–2.0×

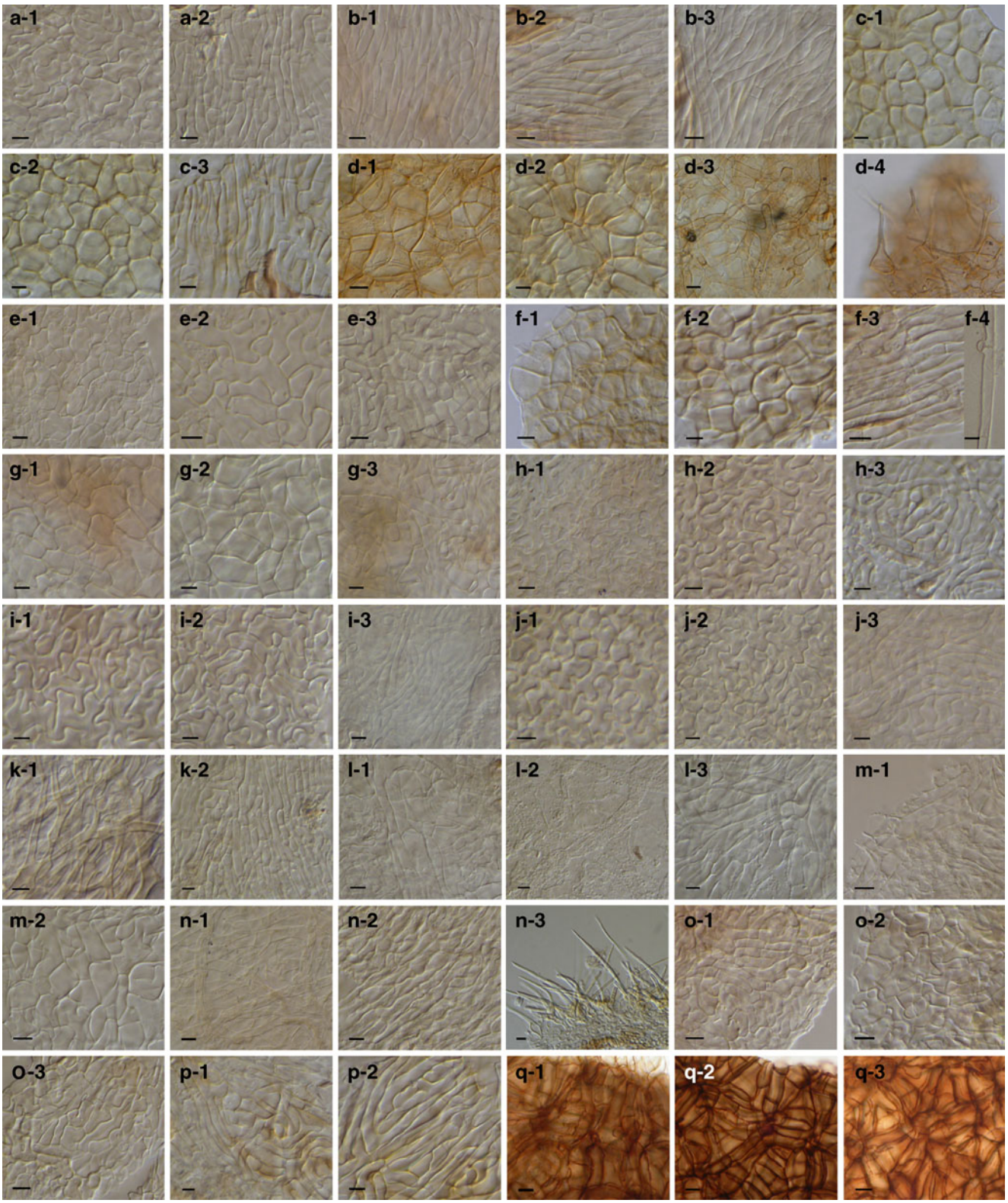
a-1
a-2
b-1
b-2
b-3
c-1
c-2
c-3
d-1
d-2
d-3
d-4
e-1
e-2
e-3
f-1
f-2
f-3
f-4
g-1
g-2
g-3
h-1
h-2
h-3
i-1
i-2
i-3
j-1
j-2
j-3
k-1
k-2
l-1
l-2
l-3
m-1
m-2
n-1
n-2
n-3
o-1
o-2
O-3
p-1
p-2
q-1
q-2
q-3

◀ **Fig. 4** Anatomical features of ectomycorrhizal mantle. **a** *Thelephora* sp.1: **a-1** Outer layer, **a-2** Inner layer; **b** *Thelephora* sp.2: **b-1** Outer layer, **b-2** Middle layer, **b-3** Inner layer; **c** *Tomentella* sp.1: **c-1** Outer layer, **c-2** Middle layer, **c-3** Inner layer; **d** *Tomentella* sp.2: **d-1** Outer layer, **d-2** Middle layer, **d-3** Inner layer, **d-4** Cystidia; **e** *Tomentella* sp.3: **e-1** Outer layer, **e-2** Middle layer, **e-3** Inner layer; **f** *Tomentella* sp.4: **f-1** Outer layer, **f-2** Middle layer, **f-3** Inner layer, **f-4** EmH; **g** *Lactarius* sp. **g-1** Outer layer, **g-2** Middle layer, **g-3** Inner layer; **h** *Russula* sp.1: **h-1** Outer layer, **h-2** Middle layer, **h-3** Inner layer; **i** *Russula* sp.2: **i-1** Outer layer, **i-2** Middle layer, **i-3** Inner layer; **j** *Russula lepida*: **j-1** Outer layer, **j-2** Middle layer, **j-3** Inner layer; **k** Russulaceae sp.: **k-1** Outer layer, **k-2** Inner layer; **l** *Boletus* sp.: **l-1** Outer layer, **l-2** Hyphal net on mantle surface, **l-3** Inner layer; **m** *Clavullina* sp.1: **m-1** Outer layer, **m-2** Inner layer; **n** *Clavulina* sp.2: **n-1** Outer layer, **n-2** Inner layer, **n-3** Cystidia; **o** Helotiales sp.1: **o-1** Outer layer, **o-2** Middle layer, **o-3** Inner layer; **p** Helotiales sp.2: **p-1** Outer layer, **p-2** Inner layer; **q** Sordariomycetes sp.: **q-1** Outer layer, **q-2** Middle layer, **q-3** Inner layer (*Bar* 5 μm)

0.16–0.25 mm (Fig. 2h, i). *Cross-section*: mantle 16–21 μm thick, including 3–5 hyphal layers, mantle cells 2–13(17)× 3–7(9) μm. Hartig's net surrounds one to two rows of cortical cells with a single chain of hyphae, hyphae 2–3 μm diam (Fig. 3h). *Mantle in plane view*: outer layers plectenchymatous, hyphae high branched forming a net-like pattern, 2–4 μm diam (Fig. 4h-1). Middle layers plectenchymatous to pseudoparenchymatous, cells irregular or subepidermoid (Fig. 4h-2). Inner layers plectenchymatous, hyphae hyline, high branched, ring-like arranged, 2–3 μm diam (Fig. 4h-3).

Russula sp.2 Morphology: solitary (not ramifying), monopodial-pinnate or monopodial-pyramidal, yellowish, surface smooth or loosely woolly, up to 3.6 mm long, 0.22–0.29 diam. Unramified ends mostly straight, tapering to the end, 0.29–1.9×0.20–0.29 mm. (Fig. 2j). *Cross-section*: mantle thin, 13–18 μm thick, comprising 3–4 hyphal layers, mantle cells 2–11×2–5 μm. Hartig's net surrounds one and a half rows of cortical cells with a single chain of elongate hyphae, *ca.* 2 μm diam (Fig. 3i). *Mantle in plane view*: outer layers pseudoparenchymatous, cells epidermoid, puzzle-like (Fig. 4i-1). Middle layers pseudoparenchymatous, cells oblong, deeply branched, subepidermoid (Fig. 4i-2). Inner layers plectenchymatous, hyphae hyline, irregularly arranged, high branched, 2–4 μm diam (Fig. 4i-3).

Russula lepida Morphology: solitary (not ramifying), monopodial-pinnate or monopodial-pyramidal, yellow-brown to red-brown, up to 5.8 mm long, main axis 0.29–0.38 mm diam. Unramified ends mostly straight, cylindrical, 0.33–2.0×0.22–0.29 mm. Mantle surface smooth (Fig. 2k). *Cross-section*: mantle 20–30(35) μm thick, mantle cells 2–15×2–6 μm. Hartig's net surrounds one row of cortical cells with one hyphal row, ca. 2 μm diam (Fig. 3j). *Mantle in plane view*: outer layers pseudoparenchymatous, cells epidermoid, puzzle-like or blunt polygonal (Fig. 4j-1). Middle layers pseudoparenchymatous, cells epidermoid (Fig. 4j-2). Inner layers plectenchymatous, hyphae hyline, irregularly arranged, high branched, 2–3 μm diam (Fig. 4j-3).

Russulaceae sp. Morphology: solitary (not ramifying), sometimes monopodial, red-brown to dark-brown, up to 0.8 mm long and 0.2 mm diam. Tips usually bent, tapering to the tip (Fig. 2l). *Cross-section*: mantle very thin, 9–13 (19) μm, mantle cells 2–13×1–3 μm. Hartig's net surrounds one row of cortical cells with a single chain of irregular and elongate hyphae, 3–6 μm diam (Fig. 3k). *Mantle in plane view*: outer layers plectenchymatous, hyphae loosely arranged and dichotomously branched, 2–3 μm diam (Fig. 4k-1). Inner layers plectenchymatous, hyphae cylindrical, branched, 2–4 μm diam (Fig. 4k-2).

Boletus sp. Morphology: monopodial-pyramidal or monopodial-pinnate, brown, surface sometimes silvery, up to 7.8 mm long, main axis 0.27–0.44 μm diam. Unramified ends bent, tapering to the tip, up to 1.7 mm long, 0.20–0.29 mm diam (Fig. 2m). *Cross-section*: mantle (32)40–55 μm thick, including 6–9 hyphal layers, mantle cells 4–20(35)×3–10 μm. Hartig's net surrounded one and a half rows of cortical cells with a single chain of hyphae, hyphae 2–3 μm diam, hyphae cells cylindrical (Fig. 3l). *Mantle in plane view*: outer layers plectenchymatous, hyphae deeply branched, embedded in a gelatinous matrix, 5–9 μm diam (Fig. 4l-1), with sparse, strongly inflated hyphae on surface (Fig. 4l-2). Inner layers plectenchymatous, hyphae irregularly arranged, 4–10 μm diam (Fig. 4l-3).

Clavulina sp.1 Morphology: monopodial or solitary (not ramifying), brown, mantle semitransparent, up to 16 mm, main axis 0.29–0.40 mm. Unramified ends slim, bent or straight, tapering to the end, up to 3.6 mm long and 0.24 mm diam (Fig. 2n). *Cross-section*: mantle 22–30(40) μm thick, including 5–7 hyphal layers, mantle cells 2–20× 2–9 μm. Hartig's net surrounds one and a half rows of cortical cells with a single chain of hyphae, hyphae 2–5 μm diam, hyphae cells roundish (Fig. 3m). *Mantle in plane view*: outer layers plectenchymatous, cells oblong or rectangular, embedded in a gelatinous matrix (Fig. 4m-1). Inner layers plectenchymatous, cells short, distinctly stout and inflated (Fig. 4m-2).

Clavulina sp.2 Morphology: irregularly monopodial, surface densely cottony, up to 6.7 mm long, main axis 0.22–0.29 mm diam, brown. Unramified ends bent, tapering to the tip, up to 1.6 mm long and 0.22 μm diam (Fig. 2o). *Cross-section*: mantle 14–27 μm thick, with 5–8 hyphal layers, mantle cells 2–15(20)×2–3 μm. Hartig's net patchy,

nest-like, one hyphal row, surrounds one to two rows of cortical cells, 2–3 μm diam (Fig. 3n, o). *Mantle in plane view*: outer layers plectenchymatous, hyphae cylindrical, branched, irregularly arranged, 3–6 μm diam (Fig. 4n-1). Inner layers plectenchymatous, hyphae embedded in a gelatinous matrix, 3–5 μm diam (Fig. 4n-2). *Cystidia*: awl-shaped, ramified, 34–83 μm long (Fig. 4n-3).

Helotiales sp.1 Morphology: monopodial-pyramidal, often in large clusters, up to 10 mm long, main axis 0.24–0.27 mm diam, yellow-brown, surfaceloosely cottony. Unramified ends mostly straight, up to 1.6 mm long and 0.16–0.2 mm diam (Fig. 2p). *Cross-section*: mantle thin, 5–15(20) μm thick, comprising 2–5 hyphal layers, mantle cells 3–17×2–5 μm. Hartig's net patchy, nest-like, one hyphal row, 2–5 μm diam (Fig. 3p). *Mantle in plane view*: outer layers plectenchymatous, hyphae deeply branched, 3–5 μm diam (Fig. 4o-1). Middle and inner layers plectenchymatous to pseudoparenchymatous, hyphae deeply branched, 3–7 μm diam (Fig. 4o-2, o-3).

Helotiales sp.2 Morphology: monopodial-pinnate, up to 8.0 mm long, ca. 0.4 mm diam, often in large clusters, brown to dark-brown, smooth. Unramified ends straight, tapering to the end, 0.53–3.6×0.24–0.29 mm (Fig. 2q). *Cross-section*: mantle (10)20–27(35) μm thick, comprising 3-8 hyphal layers, mantle cells 2–15(25)×3–5 μm. Hartig's net patchy, nest-like, one hyphal row, 2–4 μm diam (Fig. 3q). *Mantle in plane view*: outer and inner layers plectenchymatous, hyphae ring-like arranged, 3–4 μm diam (Fig. 4p-1, p-2).

Sordariomycetes sp. Morphology: fairly short, solitary (not ramifying), black, matte, usually associated with abundant debris. Tips straight or bent, 0.18–0.82×0.18–0.24 mm (Fig. 2r). *Cross-section*: mantle thin, 13–20 μm thick, comprising 2–4 hyphal layers, mantle cells 5–15×3–6 μm. Hartig's net surrounds one row of cortical cells with a single chain of irregular hyphae, ca..2 μm diam (Fig. 3r). *Mantle in plane view*: outer, middle and inner layers plectenchymatous, hyphae star-like arranged, cell walls moderately thick, melanized, 10–20×3–10 μm (Fig. 4q-1–3).

Discussion

ECM fungal community composition

Russulaceae and Thelephoraceae were the most species-rich and abundant in the ECM fungal community of *C. fargesii* in this study. Similar results of the dominant ECM fungi of Russulaceae and Thelephoraceae were reported in temperate (Ishida et al. 2009; Matsuda et al. 2009; Smith et al. 2007; Tedersoo et al. 2008) and tropical (Peay et al. 2010) forests. The other ECM fungi found in our study have been reported to form typical ECMs with plants in previous studies. For example, species of *Boletus* and *Clavulina* were common as ECM fungi in temperate (Gao and Yang 2010; Gebhardt et al. 2007; Smith et al. 2007; Tedersoo et al. 2008) and tropical (Morris et al. 2008; Peay et al. 2010; Tedersoo et al. 2007) forests. Two taxa of Sordariomycetes were reported to form ECM with *Vateriopsis seychellarum* identified by ITS and nLSU sequences in tropical forests, and their morphology and anatomical structures were described (Tedersoo et al. 2007). In addition, Sordariomycetes have been reported, using molecular techniques, to form ECM with trees of Dipterocarpaceae in a tropical rainforest of Malaysian (Peay et al. 2010) and with *Salix caprea* in a forest of Slovenia (Regvar et al. 2010). Species of Helotiales formed ECM with *Quercus douglasii*, *Nothofagus cunninghamii* and *Kobresia* spp. in temperate (Gao and Yang 2010; Morris et al. 2008; Smith et al. 2007; Tedersoo et al. 2008) and with *Quercus* spp. and Dipterocarpaceae spp. in tropical, ecosystems (Morris et al. 2008; Peay et al. 2010).

Our results indicated that a few ECM fungi were frequent and abundant, while the majority of species were rare. Similar results of a few dominant fungi in the ECM communities were reported in temperate forests (Horton et al. 2005; Ishida et al. 2009; Matsuda et al. 2009). For examples, 6 out of 13 ECM fungi detected from *Picea sitchensis* in northern England were present in more than 20% of samples (Palfner et al. 2005). *Cenococcum geophilum* and Clavulinaceae sp.1 out of 13 ECM fungal taxa were dominant in an ECM community of naturally regenerated *Pinus thunbergii* seedlings in Japan (Matsuda et al. 2009). Of the 11 ECM fungi associated with *Salix linearistipularis* in alkaline-saline soil in north China, *Geopora* sp.1 and *Tomentella* sp.1 were dominant and the other 9 fungi were rare (Ishida et al. 2009). Smith et al. (2007) found that 6 out of 92 ECM fungal species were detected in 21.3% of soil samples in a *Quercus douglasii* plot in California, USA. Furthermore, up to 80% of *Quercus rubra* roots were colonized by *C. geophilum* (Gebhardt et al. 2007). Similarly, 7 out of 44 ECM fungal taxa occupied 63.5% of total ECM root tips in a tropical *Quercus crassifolia* forest (Morris et al. 2008).

ECM morphological comparison

Thelephora spp. were reported to form ECM with many plants of Pinaceae, Betulaceae, Fagaceae, Roseceae and Salicaceae (Ingleby and Mason 1996; Ingleby et al. 1990), but only ECM morphology and anatomical structures of *Thelephora terrestris* associated with *Betula* (Ingleby et al.

1990), *Eucalyptus globulus* (Ingleby and Mason 1996), *Picea abies* (Agerer and Weiss 1989) and *Pinus patula* (Mohan et al. 1993) have been described. In this study, two *Thelephora* ECM had the same morphology and mantle structures as previous descriptions, except that the cystidia were not observed and the outer mantle layer of *Thelephora* sp.1 ECM was pseudoparenchymatous. The four *Tomentella* ECM showed diverse morphology, mantle organization, and cystidia as described in previous studies (Agerer 2006; Jakucs and Erős-Honti 2008). Of these, *Tomentella* sp. 2 resembled a previously described blackish-brown tomentelloid morphotype "*Piceirhiza nigra*" in structures (Agerer et al. 1995).

Agerer (2006) summarized anatomical characteristics of *Russula* ECM and pointed out that the ECM without cystidia had almost exclusively pseudoparenchymatous mantles and that cystidia-forming species were never pseudoparenchymatous. *Russula lepida* and *Russula* sp. 2 had the same mantle type as previous descriptions (Agerer 2006), but *Russula* sp. 1 and *Russulaceae* sp. were plectenchymatous, similar to a report by Haug et al. (2005) that *Russula puiggarii–Neea* ECM without cystidia was plectenchymatous in the outer mantle layer. Similar morphology and anatomic structures of *Lactarius* sp. ECM were observed as descriptions in UNITE (Kõljalg et al. 2005), except for lack of laticifers, as reported by Haug et al. (2005).

Morphological and anatomical characteristics of *Boletus* sp. ECM were in accordance with a previous study (Águeda et al. 2006), except that the rhizomorphs were not observed, similar to *Boletus loyo-Nothofagus* ECM described by Palfner (2001). Helotiales ECM showed similar mantle organization with ECM formed by *Phialocephala fortinii* (Helotiales) and *Populus* (Kaldorf et al. 2004), but differed in morphological characteristics (ECMs of *Phialocephala fortinii*×*Populus* were unbranched and black, whereas ECMs of Helotiales detected in this study were monopodial-branched and yellow-brown to dark-brown). Sordariomycetes sp. ECM had similar morphology and anatomical structures to the previous descriptions of two Sordariomycetes ECMs associated with *Vateriopsis seychellarum* (Tedersoo et al. 2007). A few species of *Clavulina* have been demonstrated to be ECM fungi by molecular techniques, but none was given anatomical descriptions (Smith et al. 2007; Tedersoo et al. 2008). These are the first descriptions of anatomical structures of the two *Clavulina* ECMs formed with *C. fargesii*, which had different morphology, mantle patterns, and cystidia in our study.

Acknowledgements This project is supported by the National Natural Science Foundation of China Grants (No. 30930005) and the Chinese Academy of Sciences Grant (No. KSCX2-YW-G-068).

Reference

Agerer R (1986-2006) Colour atlas of ectomycorrhizae. Einhorn, Schwäbisch Gmünd

Agerer R (2006) Fungal relationships and structural identity of their ectomycorrhizae. Mycol Prog 5:67–107. doi:10.1007/s11557-006-0505-x

Agerer R, Weiss M (1989) Studies on ectomycorrhizae. XX. Mycorrhizae formed by *Thelephora terrestris* on Norway spruce. Mycologia 81:444–453

Agerer R, Klostermeyer D, Steglich W (1995) *Piceirhiza nigra*, an ectomycorrhiza on *Picea abies* formed by a species of Thelephoraceae. New Phytol 131:377–380

Águeda B, Parlade J, de Miguel AM, Martinez-Pena F (2006) Characterization and identification of field ectomycorrhizae of *Boletus edulis* and *Cistus ladanifer*. Mycologia 98:23–30. doi:10.3852/mycologia.98.1.23

Gao Q, Yang ZL (2010) Ectomycorrhizal fungi associated with two species of *Kobresia* in an alpine meadow in the eastern Himalaya. Mycorrhiza 4:281–287. doi:10.1007/s00572-009-0287-5

Gardes M, Bruns TD (1993) ITS primers with enhanced specificity for basidiomycetes - application to the identification of mycorrhizae and rusts. Mol Ecol 2:113–118

Gardes M, Bruns TD (1996) Community structure of ectomycorrhizal fungi in a *Pinus muricata* forest: Above- and below-ground views. Can J Bot 74:1572–1583

Gebhardt S, Neubert K, Wöllecke J, Münzenberger B, Hüttl RF (2007) Ectomycorrhiza communities of red oak (*Quercus rubra* L.) of different age in the Lusatian lignite mining district, East Germany. Mycorrhiza 17:279–290. doi:10.1007/s00572-006-0103-4

Grogan P, Baar J, Bruns TD (2000) Below-ground ectomycorrhizal community structure in a recently burned bishop pine forest. J Ecol 88:1051–1062. doi:10.1046/j.1365-2745.2000.00511.x

Haug I, Weiss M, Homeier J, Oberwinkler F, Kottke I (2005) Russulaceae and Thelephoraceae form ectomycorrhizas with members of the Nyctaginaceae (Caryophyllales) in the tropical mountain rain forest of southern Ecuador. New Phytol 165:923–936. doi:doi:10.1111/j.1469-8137.2004.01284.x

Horton TR, Bruns TD (2001) The molecular revolution in ectomycorrhizal ecology: peeking into the black-box. Mol Ecol 10:1855–1871. doi:10.1046/j.0962-1083.2001.01333.x

Horton TR, Molina R, Hood K (2005) Douglas-fir ectomycorrhizae in 40-and 400-year-old stands: mycobiont availability to late successional western hemlock. Mycorrhiza 15:393–403. doi:10.1007/s00572-004-0339-9

Ingleby K, Mason PA (1996) Ectomycorrhizas of *Thelephora terrestris* formed with *Eucalyptus globulus*. Mycologia 88:548–553

Ingleby K, Mason PA, Last FT, Fleming LV (1990) Identification of ectomycorrhizas. HMSO, London

Ishida TA, Nara K, Ma SR, Takano T, Liu SK (2009) Ectomycorrhizal fungal community in alkaline-saline soil in northeastern China. Mycorrhiza 19:329–335. doi:10.1007/s00572-008-0219-9

Jakucs E, Erős-Honti Z (2008) Morphological-anatomical characterization and identification of *Tomentella* ectomycorrhizas. Mycorrhiza 18:277–285. doi:10.1007/s00572-008-0183-4

Kõljalg U, Larsson KH, Abarenkov K, Nilsson RH, Alexander IJ, Eberhardt U, Erland S, Høiland K, Kjøller R, Larsson E, Pennanen T, Sen R, Taylor AFS, Tedersoo L, Vralstad T, Ursing BM (2005) UNITE: a database providing web-based methods for the molecular identification of ectomycorrhizal fungi. New Phytol 166:1063–1068. doi:10.1111/j.1469-8137.2005.01376.x

Kaldorf M, Renker C, Fladung M, Buscot F (2004) Characterization and spatial distribution of ectomycorrhizas colonizing aspen

clones released in an experimental field. Mycorrhiza 14:295–306. doi:10.1007/s00572-003-0266-1

Liang Y, Guo LD, Du XJ, Ma KP (2007) Spatial structure and diversity of woody plants and ectomycorrhizal fungus sporocarps in a natural subtropical forest. Mycorrhiza 17:271–278. doi:10.1007/s00572-006-0096-z

Matsuda Y, Noguchi Y, Ito S (2009) Ectomycorrhizal fungal community of naturally regenerated *Pinus thunbergii* seedlings in a coastal pine forest. J For Res 14:335–341. doi:10.1007/s10310-009-0140-x

Mohan V, Natarajan K, Ingleby K (1993) Anatomical studies on ectomycorrhizas. I. the ectomycorrhizas produced by *Thelephora* terrestris on *Pinus patula*. Mycorrhiza 3:39–42

Morris MH, Perez-Perez MA, Smith ME, Bledsoe CS (2008) Multiple species of ectomycorrhizal fungi are frequently detected on individual oak root tips in a tropical cloud forest. Mycorrhiza 18:375–383. doi:10.1007/s00572-008-0186-1

Palfner G (2001) Taxonomische studien an ektomykorrhizen aus den Nothofagus-Wäldern Mittelsüdchiles. Bibliotheca Mycologica 190

Palfner G, Casanova-Katny MA, Read DJ (2005) The mycorrhizal community in a forest chronosequence of Sitka spruce [*Picea sitchensis* (Bong.) Carr.] in Northern England. Mycorrhiza 15:571–579. doi:10.1007/s00572-005-0364-3

Peay KG, Kennedy PG, Davies SJ, Tan S, Bruns TD (2010) Potential link between plant and fungal distributions in a dipterocarp rainforest: community and phylogenetic structure of tropical ectomycorrhizal fungi across a plant and soil ecotone. New Phytol 185:529–542. doi:10.1111/j.1469-8137.2009.03075.x

Peter M, Ayer F, Cudlin P, Egli S (2008) Belowground ectomycorrhizal communities in three Norway spruce stands with different degrees of decline in the Czech Republic. Mycorrhiza 18:157–169. doi:10.1007/s00572-008-0166-5

Regvar M, Likar M, Piltaver A, Kugoni N, Smith JE (2010) Fungal community structure under goat willows (*Salix caprea* L.) growing at metal polluted site: the potential of screening in a model phytostabilisation study. Plant Soil 330:345–356. doi:10.1007/s11104-009-0207-7

Simard SW, Perry DA, Jones MD, Myrold DD, Durall DM, Molina R (1997) Net transfer of carbon between ectomycorrhizal tree species in the field. Nature 388:579–582

Smith ME, Douhan GW, Rizzo DM (2007) Ectomycorrhizal community structure in a xeric *Quercus* woodland based on rDNA sequence analysis of sporocarps and pooled roots. New Phytol 174:847–863. doi:doi:10.1111/j.1469-8137.2007.02040.x

Smith SE, Read DJ (2008) Mycorrhizal symbiosis. Academic, San Diego

Tedersoo L, Suvi T, Beaver K, Kõljalg U (2007) Ectomycorrhizal fungi of the Seychelles: diversity patterns and host shifts from the native *Vateriopsis seychellarum* (Dipterocarpaceae) and *Intsia bijuga* (Caesalpiniaceae) to the introduced *Eucalyptus robusta* (Myrtaceae), but not *Pinus caribea* (Pinaceae). New Phytol 175:321–333. doi:10.1111/j.1469-8137.2007.02104.x

Tedersoo L, Jairus T, Horton BM, Abarenkov K, Suvi T, Saar I, Koljalg U (2008) Strong host preference of ectomycorrhizal fungi in a Tasmanian wet sclerophyll forest as revealed by DNA barcoding and taxon-specific primers. New Phytol 180:479–490. doi:10.1111/j.1469-8137.2008.02561.x

Wang Q, Guo LD (2010) Ectomycorrhizal community composition of *Pinus tabulaeformis* assessed by ITS-RFLP and ITS sequences. Botany 88:590–595

White T, Bruns T, Lee S, Taylor J (1990) Amplification and direct sequencing of fungal ribosomal RNA genes for phylogenetics. In: Innis MA, Gelfand DH, Sninsky JJ, White TJ (eds) PCR protocols: a guide to methods and application. Academic, San Diego, pp 315–322